Bose-fermi mixtures in a three-dimensional optical lattice

Liu, Qingmei; Dai, Xi; Fang, Zhong; Zhuang, Jia Ning; Zhao, Yang

2010

Liu, Q. M., Dai, X., Fang, Z., Zhuang, J. N., & Zhao, Y. (2010). Bose-Fermi Mixtures in a Three-Dimensional Optical Lattice. Applied Physics B: Lasers and Optics, 99, 639-654.

https://hdl.handle.net/10356/94323

https://doi.org/10.1007/s00340-010-4074-y

Appl Phys B manuscript No.
(will be inserted by the editor)

Bose-fermi mixtures in a three-dimensional optical lattice

Qing-Mei Liu[1,2], Xi Dai[2], Zhong Fang[2], Jia-Ning Zhuang[2], and Yang Zhao[1] ⋆

[1]School of Materials Science and Engineering, Nanyang Technological University, Singapore 639798

[2]Institute of Physics, Chinese Academy of Sciences, Beijing 100080, China

January 25, 2010

Abstract Using the dynamical mean field theory and the Gutzwiller method, we study the Mott transition in bose-fermi mixtures confined in a three-dimensional optical lattice and analyze the effect of fermions on the coherence of bosons. We conclude that increasing fermion composition reduces bosonic coherence in the presence of strong bose-fermi interactions and under the condition of the integer filling factors for composite fermions, which consist of one fermion and one or more bosonic holes. Various phases of the mixtures have been demonstrated including phase separation of two species, coexisting regions of superfluid bosons and fermionic liquids, and Mott regions in the phase space spanned by the chemical potentials of the bosons and the fermions.

PACS: 03.75.Kk, 73.43.Nq, 05.30Fk

⋆ *Corresponding author:* Address: School of Materials Science and Engineering Division of Materials Science Block N4.1, Level 1, Room 01, 50 Nanyang Ave Nanyang Technological University Singapore 639798; Telephone: +65 6513 7990; Fax: +65 6790 9081; E-mail: yzhao@ntu.edu.sg

1 Introduction

Quantum statistics plays a very important role in determining various physical properties of quantum fluids at low temperatures. For a purely bosonic system, the Bose-Einstein condensation can be found in the ground state, while for a pure fermionic system, usually a fermi surface in the momentum space appears, within which the states are fully occupied. On the other hand, more and more novel quantum many-body phenomena in condensed matter physics, such as the Mott-transition in bosonic systems and BCS-like superfluid transitions in fermionic systems, have been predicted and observed [1–4] by trapping ultracold atoms in optical lattices. Moreover, a new type of quantum fluids with both bosonic and fermionic atoms can now be constructed. Since one can tuned experimentally the ratio of the two types of atoms, the effective interactions among those atoms as

well as the total filling factor of the lattice, the phase diagram of the bose-fermi mixture can be made very rich. And it has become a good testing ground to study the role of the quantum statistics in various quantum phases.

Quite a few novel quantum phases, such as the composite fermions, charge-density waves, spin glass and supersolid [5,6], have been predicted for bose-fermi mixtures in an optical lattice. Very recently, important progress has been made experimentally on understanding the effect of fermionic species on the phase coherence of bosonic atoms in optical lattices [7,8]. It was observed that adding fermions can result in the loss of phase coherence of bose gases. In order to explain this experimental finding, one obvious argument is that higher order effects such as induced effective interactions between the bosons can lead to an increase in the bosonic visibility in a one-dimensional model independent of the sign of bose-fermi interactions [9]. Another viewpoint attributes the possible cause to the temperature effects [10]. E.g., increased temperature is proposed to reduce the coherence of the bose gas when ramping-up the optical lattice in an experimental procedure. At present, much contention still surrounds the issue [11,12]. Among many factors affecting the role of the fermionic atoms, we will focus on the filling factors of the bosons and the fermions. If the filling factor of bosonic atoms is an integer number per lattice site and the repulsion between two species of atoms is strong enough, adding fermionic atoms will push some bosonic atoms away from their original positions, facilitating the formation of superfluid states. While all fermions are bound with one or more bosons or bosonic holes, the presence of fermionic atoms has two consequences. First, replacing some bosonic atoms with fermionic ones will introduce bosonic holes to the system analogous to doping the Mott insulator with holes, and thus enhance the superfluid phase. Second, the fermionic atoms in the system can be also viewed as scattering centers of the bosons, which tend to destroy superfluidity. Therefore, if the repulsive interaction between the two species is weak, the former effect is dominant and superfluidity will be enhanced by replacing some bosons with fermions; if the interaction is strong enough, the latter effect will dominate and superfluidity will be suppressed.

In this work, we will discuss extensively the effects of fermions on the bose gases, and explore possible novel quantum phases for many-body systems with mixed statistics by applying the dynamical mean field theory (DMFT) [13] and the Gutzwiller approximation [14]. The DMFT method is a newly developed many-body technique, which maps lattice models to corresponding quantum impurity models subject to self-consistency conditions. Beyond the static mean field approaches, DMFT keeps the full local dynamics induced by local interactions. DMFT is also capable to interpolate between band-like and atomic-like behavior of electrons. Therefore it is a powerful numerical technique to study the Mott transition in strongly correlated electronic systems. On the other hand, the Gutzwiller approximation is an effec-

tive variational scheme for the ground state studies of many important phenomena, such as the Mott transition, ferromagnetism and superconductivity. It was first proposed by Gutzwiller to study itinerant ferromagnetism in systems with partially filled d bands (described by the Hubbard Model [15]). In this approach, a many-body trial wave function was constructed so that the weight of atomic configurations can be adjusted by varying the variational parameters. Both itinerant and atomic features can be described by this type of Gutzwiller wave functions. Thus, a unified description for correlated systems can be built by the Gutzwiller method. There have also been various techniques, e.g., combining with DMFT and the local density approximation(LDA), to extend the application of the Gutzwiller approach [19]. The zero-order approximation of the Gutzwiller method is equivalent to the widely-used slave-boson approach, but our implementation of the Gutzwiller approximation includes a full set of variational parameters, which is computationally more demanding and yields more accurate results. Other approaches used for Bose-Fermi mixtures, Bose-Hubbard and Fermi-Hubbard systems include exact diagonalization[16], Bethe ansatz [17], and quantum Monte Carlo [18], which are often applied to one-dimensional systems.

The paper is organized as follows. In Sec. II we introduce the DMFT approach and related numerical techniques. In Sec. III, we first consider a homogeneous case for the bose-fermi mixtures in a three-dimensional periodical optical lattice. We discuss the quantum phase transition of the two species for a limiting case of infinitely large repulsive bose-bose interactions and the general case of finite bose-bose interactions. Furthermore, we analyze the effect of the fermion concentration and interspecies interactions on the occurrence of the superfluid-Mott transition of bosons, and make comparison with the experimental results. In the presence of a slowly external potential, we give the general phase diagram of the mixture and display the particle distribution. Conclusions are drawn in Sec. IV.

2 Methodology

2.1 DMFT

In order to describe an interacting bose-fermi mixture in an optical lattice, we adopt the tight-binding Hubbard model from Ref. [20]. It is assumed that the temperature is low enough to achieve degeneracy and the optical potential wells are sufficiently deep so that the atoms only occupy the lowest band. The fermions are supposed to be polarized in this model. In this section we confine ourselves to discussions of the homogeneous case in the absence of an external trapping potential. The Hamiltonian reads:

$$\hat{H} = \hat{H}_{\mathrm{b}} + \hat{H}_{\mathrm{f}} + \hat{H}_{\mathrm{bf}}$$

$$\hat{H}_{\mathrm{b}} = -t_{\mathrm{b}} \sum_{i,j} b_i^{\dagger} b_j + \frac{U_{\mathrm{bb}}}{2} \sum_i n_{\mathrm{b}i}(n_{\mathrm{b}i} - 1) - \mu_{\mathrm{b}} \sum_i n_{\mathrm{b}i}$$

$$\hat{H}_{\mathrm{f}} = -t_{\mathrm{f}} \sum_{i,j} f_i^{\dagger} f_j - \mu_{\mathrm{f}} \sum_i n_{\mathrm{f}i}$$

$$\hat{H}_{\rm bf} = U_{\rm bf} \sum_i n_{{\rm b}i} n_{{\rm f}i} \quad (1)$$

where subscripts f and b denote fermionic and bosonic species, respectively, $f_i^\dagger$ ($b_i^\dagger$) is the fermionic (bosonic) creation operator at site i, and $n_{{\rm b}i} = b_i^\dagger b_i$ ($n_{{\rm f}i} = f_i^\dagger f_i$) is the occupation number operator for bosons (fermions) on site i. $H_{\rm b}$ ($H_{\rm f}$) represents the purely bosonic (fermionic) Hamiltonian. $H_{\rm bf}$ gives the boson-fermion on-site interactions. $U_{\rm bb}$ and $U_{\rm bf}$ represent the boson-boson on-site interactions and the boson-fermion interactions, respectively. They can be tuned by controlling the laser intensity of the optical lattice in the experiments. According to the results of the mean field theory, the repulsive $U_{\rm bf}$ can lead to the phase separation between the fermions and the bosons, while the attractive $U_{\rm bf}$ triggers a system collapse above a critical boson number. Here we concentrate on the case of repulsive bose-fermi interactions with an equal hopping strength for bosons and fermions ($t_{\rm b} = t_{\rm f}$). However, results obtained in this paper can also be applied to a similar fermion-boson system with attractive interactions [21] thanks to the existence of a mapping using particle-hole transformation on the fermions.

We treat the bosons by the mean-field approximation (MFA) and the fermions by DMFT, which was first developed and applied to the same system by Titvinidze, Snoek and Hofstetter [22]. For bosons, in the framework of the static MFA, the dynamics of the superfluid order parameter is not accounted for, and the investigation on the dynamics of boson degrees of freedoms by DMFT can be referred to Ref. [23]. Following Ref. [24], $\langle b_i^\dagger \rangle = \langle b_i \rangle = \phi$ is defined as the superfluid order parameter. After decoupling the hopping term, the Hamiltonian $H_{\rm b}$ is simplified as

$$\begin{aligned} \hat{H}_{\rm b} = & \sum_i \left[-z t_{\rm b} (\phi b_i^\dagger + \phi b_i - |\phi|^2) \right] \\ & + \sum_i \left[\frac{U_{\rm bb}}{2} n_{{\rm b}i} (n_{{\rm b}i} - 1) - \mu_{\rm b} n_{{\rm b}i} \right] \end{aligned} \quad (2)$$

It is noted that the mean-field decoupling approximation underestimates the superfluid order parameter ϕ.

The momentum-space representation of $\hat{H}_{\rm f}$ reads

$$\begin{aligned} \hat{H}_{\rm f} &= \sum_k (\varepsilon_k - \mu_{\rm f}) c_k^\dagger c_k \\ \varepsilon_k - \mu_{\rm f} &= -2t_{\rm f} [\cos k_x a + \cos k_y a + \cos k_z a] \end{aligned} \quad (3)$$

where the lattice spacing a is set to 1, and ε_k denotes the dispersion of non-interacting fermions in the three-dimensional cubic lattice. Under DMFT, the lattice model can be mapped onto a single impurity Anderson model (SIAM). With all energy terms rescaled by $z t_{\rm b}$, the reduced impurity Hamiltonian reads:

$$\begin{aligned} \hat{H}^{\rm simp} = & -\mu_{\rm f} n_{\rm f} + \sum_l \epsilon_l c_l^\dagger c_l + \sum_l v_l (c_l^\dagger f + f^\dagger c_l) \\ & -(b^\dagger \phi + \phi b - |\phi|^2) + \frac{U_{\rm bb}}{2} n_{\rm b} (n_{\rm b} - 1) \\ & -\mu_{\rm b} n_{\rm b} + U_{\rm bf} n_{\rm b} n_{\rm f} \end{aligned} \quad (4)$$

where v_l describes the couplings between the local impurity states and the associated bath, ϵ_l represents the dispersion of the electrons in the bath, and f (b) denotes the local fermi (bose) operator.

Now we can define the impurity Green's function $G^{\rm imp}$ as

$$G^{\rm imp}(\omega) = \frac{1}{\omega - \hat{H}^{\rm simp}} \tag{5}$$

When the set of coupling parameters $\{\epsilon_l, v_l\}$ is initially chosen, the impurity Green's function $G^{\rm imp}$ and the self-energy function $\Sigma^{\rm loc}$ are numerically evaluated by the exact diagonalization method. By substituting $\Sigma^{\rm loc}$ into the Dyson eqnarray, the local Green's function $G_{\rm lattice}$ can be obtained by

$$G_{\rm lattice}(\omega) = \frac{1}{N}\sum_k \frac{1}{\omega + \mu_{\rm f} - \varepsilon_k - \Sigma^{\rm loc}(\omega)} \tag{6}$$

Consequently, one can get an updated Weiss function G_0

$$G_0^{-1}(\omega) = G^{-1}_{\rm lattice}(\omega) + \Sigma^{\rm loc}(\omega) \tag{7}$$

In the numerical implementation, we approximate the Weiss function G_0 by a function $G_0^{\rm simp}$ with a finite number N_c of sites. Then the standard conjugate gradient method is used to locate the functional minimum d with respect to $\{\epsilon_l, v_l\}$[13]:

$$\begin{aligned} d &= \frac{1}{N_{\rm max}+1}\sum_{n=1}^{N_{\rm max}} |G_0(i\omega)^{-1} - G_0^{\rm simp}(i\omega)^{-1}|^2 \\ G_0^{\rm simp}(i\omega)^{-1} &= i\omega + \mu_{\rm f} - \sum_{l=1}^{l=N_c}\frac{v_l^2}{i\omega - \epsilon_l} \end{aligned} \tag{8}$$

For a theoretical investigation of the Anderson model, it is efficient to map the Hamiltonian onto a linear chain. The fermions in this case can be identified as conducting electrons. The mapping results in a representation of the SIAM as a semi-infinite tight-binding chain with nearest-neighbor hopping only and the impurity at one end of the chain [25]. In Eq. (4), the creation operators $c_l^\dagger$ of the conduction electrons are directly coupled to the impurity via the hybridization v_l. Now the creation operators $c_l^\dagger$ are superposed to form a new operator $c_1^\dagger$,

$$\begin{aligned} c_1^\dagger &= \frac{1}{V}\sum_l v_l c_l^\dagger \\ V^2 &= \sum_l |v_l|^2 \end{aligned} \tag{9}$$

where $c_1^\dagger$ creates a localized one-electron state on the first site of the conduction electron chain $|1\rangle = c_1^\dagger|0\rangle$, when $|0\rangle$ is a Fock vacuum state. V describes the coupling strength between the local state and the first site along the transformed semi-infinite chain. With $c_1^\dagger$ and c_1, the hybridization term in the Eq. (4) can be written as

$$\sum_l v_l(c_l^\dagger f + f^\dagger c_l) = V(f^\dagger c_1 + c_1^\dagger f). \tag{10}$$

The contribution from the electron bath ($\hat{H}_c = \sum_l \epsilon_l c_l^\dagger c_l$) to the total Hamiltonian [*cf. Eq.* (4)] is transformed using a Lanczos tridiagnalization procedure. A new single-particle basis for the electron bath starting from the state $|1\rangle$ is constructed. Then a sequence of new basis states can be constructed by applying a Schmidt orthogonalization to $|1\rangle$, $\hat{H}_c|1\rangle$, $\hat{H}_c^2|1\rangle$, $\cdots$. Thus, the Hamiltonian $\hat{H}_c$ is tridiagonal in the new Schmidt basis. In the second quantized form it becomes a tight-binding linear chain with nearest-neighbor hopping only [25].

In the DMFT simulation, the initial Weiss function G_0 is obtained by calculating the lowest energy band of non-interacting spinless fermions in a cubic lattice, and the width of the energy band is chosen as $2t_{\rm f}$. The exact diagonalization method is used as the impurity solver to

obtain the finite temperature Green's function, wherein a low effective temperature $1/T = 200$ is introduced.

2.2 The Gutzwiller method

In this subsection, we employ the Gutzwiller variational approach to investigate the bose-fermi mixtures. The Gutzwiller approach is one of the simplest ways to study electronic correlations in many-body systems. Compared with DMFT, the Gutzwiller method is a relatively uncomplicated approach, but one nonetheless effective to capture the low-energy physics of the strongly correlated systems. With the bosonic hopping term treated by the mean-field approximation, the Hamiltonian (1) can be written in two terms

$$\begin{aligned}
\hat{H} &= \hat{H}_{\rm hop} + \hat{H}_{\rm loc} \\
\hat{H}_{\rm loc} &= \sum_i (U_{\rm bf} n_{{\rm b}i} n_{{\rm f}i} - \mu_{\rm f} n_{{\rm f}i} - \mu_{\rm b} n_{{\rm b}i}) + \\
&\quad \sum_i [-z t_{\rm b} (b_i^\dagger \phi + \phi b_i - |\phi|^2) \\
&\quad + \frac{U_{\rm bb}}{2} n_{{\rm b}i}(n_{{\rm b}i} - 1)] \\
\hat{H}_{\rm hop} &= -t_{\rm f} \sum_{i,j} f_i^\dagger f_j
\end{aligned} \tag{11}$$

Due to the pure density correlation in the local interactions $\hat{H}_{\rm loc}$, we can always diagonalize $\hat{H}_{\rm loc}$ in the atomic configuration representation [14]:

$$\hat{H}_{\rm loc} = \sum_i \sum_\Gamma E_\Gamma \widehat{m}_{i\Gamma} \tag{12}$$

where $\widehat{m}_\Gamma$ is the projection operator onto configuration $|\Gamma\rangle$, and all configurations $\{|\Gamma\rangle\}$ form a locally complete basis set.

In Eq. (11), if the interactions are absent, the ground state can be solved exactly by the uncorrelated Hartree wave function $|\varphi_0\rangle$, which is a single determinant of single-particle wave functions. However, in the presence of interaction terms, $|\varphi_0\rangle$ is no-longer a good approximation due to its many energetically unfavorable configurations. The Gutzwiller wave function $|\psi_G\rangle$ is constructed by applying a many-particle projection operator on $|\varphi_0\rangle$

$$|\psi_G\rangle = \mathcal{P}|\varphi_0\rangle = \prod_i \sum_\Gamma \lambda_\Gamma \widehat{m}_{i\Gamma} |\varphi_0\rangle \tag{13}$$

where λ_Γ denotes variational parameters modifying projection weights on the local configurations. The projection operator $\mathcal{P}$ adjusts the weight of each configuration through the variational parameters λ_Γ. According to above definition, the expectation value of the Hamiltonian (11) is written as

$$E = \langle H \rangle = \frac{\langle \Psi_G | \hat{H} | \Psi_G \rangle}{\langle \Psi_G | \Psi_G \rangle} = \frac{\langle \varphi_0 | \hat{\mathcal{P}} \hat{H} \hat{\mathcal{P}} | \varphi_0 \rangle}{\langle \varphi_0 | \hat{\mathcal{P}}^2 | \varphi_0 \rangle} \tag{14}$$

Then the variational energy can be explicitly evaluated as

$$\begin{aligned}
E &= Z_{\rm f} \cdot \widetilde{\epsilon_0} + \sum_\mu E_\mu m_\mu + \phi^2 \\
\sqrt{Z_{\rm f}} &= \frac{1}{\sqrt{n_{\rm f}(1-n_{\rm f})}} \sum_{\mu\nu} \sqrt{m_\mu m_\nu} \cdot \delta_{n_{{\rm f},\mu}, n_{{\rm f},\nu}+1} \\
\phi &= \sum_{\mu\nu} \sqrt{m_\mu m_\nu} \cdot \delta_{n_{{\rm b},\mu}, n_{{\rm b},\nu}+1} \cdot \sqrt{n_{{\rm b},\nu}}
\end{aligned} \tag{15}$$

$$\widetilde{\epsilon_0} = \langle f_i^\dagger f_j \rangle_0 \tag{16}$$

Here m_μ denotes the atomic configuration weight, and the quasi-particle weight $Z_{\rm f}$ is a characteristic quantity describing the strength of the correlation between fermions, The quantity $\widetilde{\epsilon_0}$ can be interpreted as the kinetic energy of the non-interacting fermions.

It has been shown that the zeroth order approximation of the Gutzwiller method is equivalent to the well-known slave boson approach [26,27]. For the aforementioned Hamiltonian, we can introduce a set of slave boson operators $l_\mu^\dagger(\mu = 0, 1)$, which denotes, respectively, projection operators onto the empty and singly occupied state for each site [26]. Then the electron operators can be expressed in terms of the pseudo fermion $a_i^\dagger$ and slave bosons:

$$\begin{aligned} f_i^\dagger &= z_i^\dagger a_i^\dagger \\ z_i^\dagger &= \frac{1}{\sqrt{n_\mathrm{f}(1-n_\mathrm{f})}} \sum_{\mu\nu} [D_{\mu\nu}]^* l_\mu^\dagger l_\nu \end{aligned} \tag{17}$$

where $D_{\nu\mu} = \langle\nu| f |\mu\rangle$ is the matrix element of the electron operator represented in terms of the local atomic states, and $z_i^\dagger$ describes the change in the slave-boson occupation number[28]. Consequently, the original Hamiltonian can be written in terms of the slave particles as

$$\hat{H}_\mathrm{slave} = -t_\mathrm{f} \sum_{i,j} a_i^\dagger a_j z_i^\dagger z_j + \sum_{i,\mu} E_\mu l_\mu^\dagger l_\mu \tag{18}$$

Within the mean-field approach, all the slave boson operators are treated as c-numbers, following which the ground state energy can be determined iteratively under the local constraints [27]

$$\begin{aligned} \sum_\mu l_\mu^\dagger l_\mu &= 1 \\ \sum_\mu \eta_\mu l_\mu^\dagger l_\mu &= a_i^\dagger a_i \\ \eta_\mu &= \sum_\nu D_{\nu\mu}^* D_{\nu\mu} \end{aligned} \tag{19}$$

where η_μ is the average particle number for the configuration μ.

3 Results and Discussions

3.1 The Mott transition

Since the transition from superfluid to the Mott insulator in a purely bosonic system was experimentally observed, quantum phase transitions in cold-atom systems have become a paradigm for studying many-body phenomena in strongly correlated systems. Here, we first derive a general condition for the occurrence of the Mott phase transition for the bose-fermi mixture. In the case of vanishing bose and fermi hopping integrals, $t_\mathrm{f} = t_\mathrm{b} = 0$, the ground state of the mixture system is highly degenerate. This means that there are many possible configurations for bosons and fermions in the ground state. Furthermore, if these degenerate states remain stable when the hopping terms are taken into account as a first order perturbation, then it is favored to form a Mott state. It follows that the average occupation numbers of boson and fermion satisfy $M \times n_\mathrm{f} + N \times (1 - n_\mathrm{f}) = n_\mathrm{b}$, where M and N are both arbitrary integer numbers. This identity is a general condition for the Mott phase transition of the bose-fermi mixture in a periodical optical lattice.

After obtaining the general condition of the Mott phase transition, we then focus on a special case with $n_\mathrm{b} + n_\mathrm{f} = 1$. First of all, we discuss the quantum phase transition of a limiting case in which $U_\mathrm{bb} \to +\infty$, and the bosonic occupation number is only allowed to be zero or one (the so-called hard-core or Tonks bosons [29]). Neglecting the constant terms, the Hamiltonian has the

following form:

$$H^{\rm simp} = \sum_l \epsilon_l c_l^\dagger c_l + \sum_l v_l (c_l^\dagger f + f^\dagger c_l) - \phi(b^\dagger + b) + U_{\rm bf}(n_{\rm b} - 1/2)(n_{\rm f} - 1/2) \quad (20)$$

It is obviously from Eq. (20) that the bosons and fermions have particle-hole symmetry when $\phi = 0$, and the ground state has a two-fold degeneracy. In fact, even for nonzero ϕ, the result indicates that the mixture still has well-defined particle-hole symmetry. When $U_{\rm bb} \to +\infty$, it is impossible for two or more bosons occupying the same lattice site, which is analogous to the Pauli exclusion principle for fermions, causing the bosons to exhibit fermion-like properties. Therefore the Tonks bosons are also called fermionized Bose gases. There have been efforts to prepare the Tonks-Girardeau gases in one-dimensional optical lattices [30]. For the mixed system, only one boson is allowed on one site together with one fermion or a fermionic hole. Fig. 1 shows the superfluid order parameter as a function of $U_{\rm bf}$ calculated with the method of exact diagonalization. It can be seen that with increasing $U_{\rm bf}$ the superfluid state is converted into the Mott insulator state. The critical value of $U_{\rm bf}$ is about 2.9, comparable to that in the Mott-insulator transition of a fermionic system with spins. After the superfluid-Mott transition, the fermions also form a Mott state at the same critical value $U_{\rm bf}^c$, as shown in Fig. 2.

Next, a more realistic case with finite $U_{\rm bb}$ is discussed. In order to demonstrate the effect of the fermion composition in the mixture, we adopt equal values for

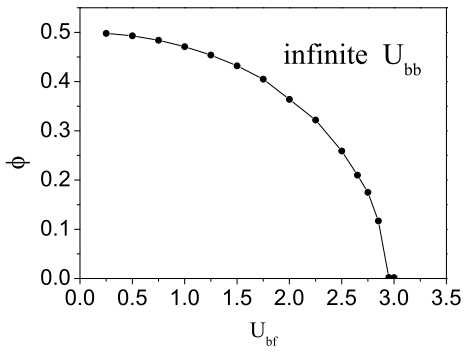

Fig. 1 The superfluid order parameter ϕ as a function of boson-fermion interaction $U_{\rm bf}$ calculated for $U_{\rm bb} \to +\infty$ and via exact diagonalization.

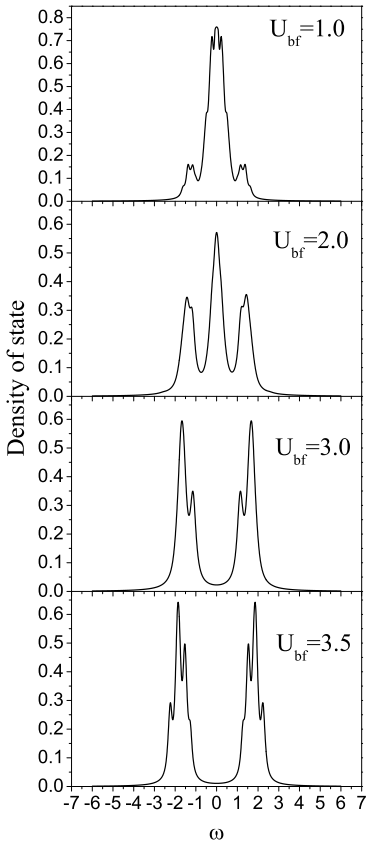

Fig. 2 Fermion density of states at the fermi energy level calculated by DMFT for $U_{\rm bb} \to +\infty$ and four values of $U_{\rm bf}$: $1.0, 2.0, 3.0$ and 3.5.

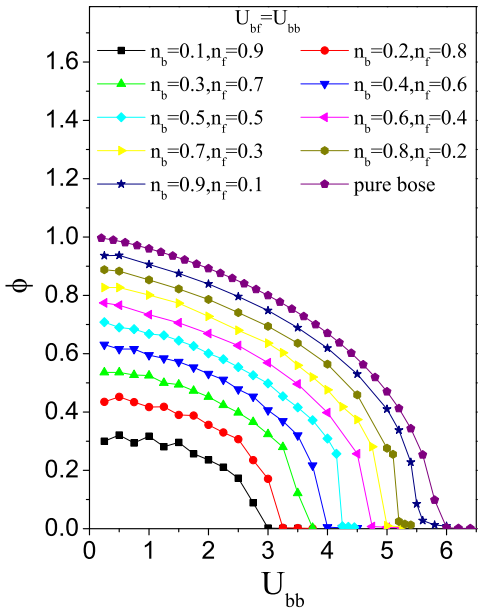

Fig. 3 The superfluid order parameter ϕ as a function of the boson-boson interaction strength $U_{\rm bb}$ for various boson-fermion compositions. The boson-fermion interaction strength $U_{\rm bf}$ is fixed to the same value as $U_{\rm bb}$: $U_{\rm bf} = U_{\rm bb}$.

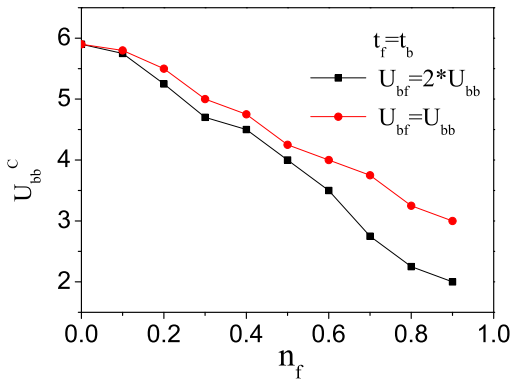

Fig. 4 The critical point of the superfluid-insulator transition as a function of the fermion composition with $U_{\rm bf} = U_{\rm bb}$ and $U_{\rm bf} = 2U_{\rm bb}$. The results are qualitatively consistent with Ref. [8].

$U_{\rm bf}$ and $U_{\rm bb}$. The total filling factor for bosons and fermions is set to be 1 such that there is one fermion for each bosonic hole in the Mott-insulator state. In the absence of fermions, the Mott transition is known to occur at a critical value of the bose-bose coupling $U^c_{\rm bb} = 5.8$ for an average number of one atom per site in three dimensions [31]. Note that here the $U^c_{\rm bb}$ has been scaled by $zt_{\rm b}$ when deriving the impurity Hamiltonian in Eq. (4). When a few bosons are replaced by fermions, the critical value $U^c_{\rm bb}$ for the superfluid-Mott transition decreases. As clearly shown in Fig. 3, the critical value decreases monotonically upon increasing the composition of fermions in the mixture. From Fig. 3, it can also be seen that with half of bosons replaced by fermions, the quantum critical value is reduced to $U^c_{\rm bb} = 4.2$. Due to adequate bose-fermi interactions, added fermions can bind with bosonic holes and suppress the motion of bosons, resulting in a loss of bosonic phase coherence. To clearly demonstrate the shift of the critical value of the Mott transition, we plot $U^c_{\rm bb}$ as a function of the fermion composition for the case of $U_{\rm bf} = U_{\rm bb}$ and $U_{\rm bf} = 2U_{\rm bb}$ in Fig. 4. These results agree qualitatively with Ref. [8], in which it was found that addition of fermions significantly decreases bosonic coherence.

In addition, with the disappearance of superfluid state of the bosons, the fermions in the mixture also undergo a quantum phase transition. In the absence of the bosons, the spinless fermions only have hopping terms, and the metallic state is easily distinguished from the Mott state

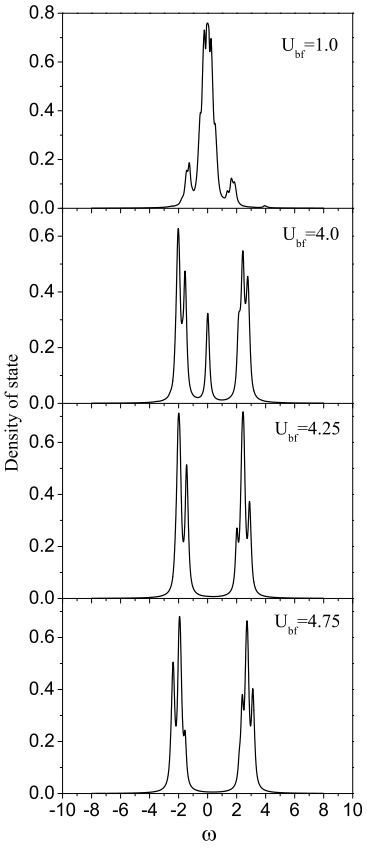

Fig. 5 Fermion density of states calculated by DMFT for $n_{\rm f} = n_{\rm b} = 0.5$ and $U_{\rm bb} = U_{\rm bf}$. Four values of $U_{\rm bf}$: 1.0, 4.0, 4.25 and 4.75, are shown.

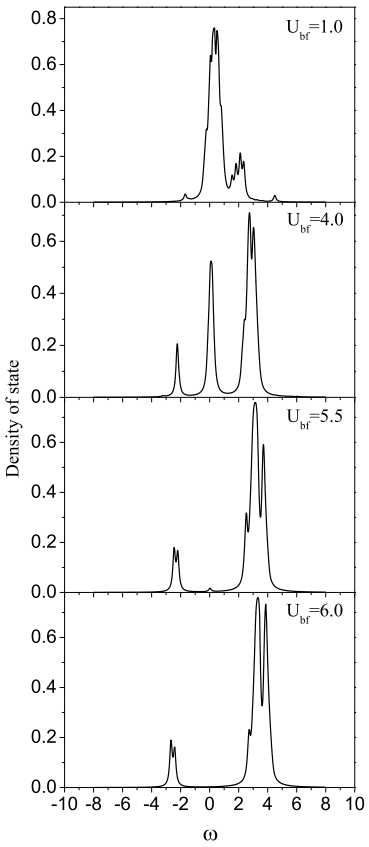

Fig. 6 Fermion density of states for fermions calculated by DMFT for $n_{\rm f} = 0.1$, $n_{\rm b} = 0.9$ and $U_{\rm bb} = U_{\rm bf}$. Four values of $U_{\rm bf}$, 1.0, 4.0, 5.5 and 6.0, are shown.

with at most one fermion occupying each lattice site. For the bose-fermi mixtures, the metal-insulator phase transition for fermions closely depends on the tunneling strength, the total filling factor and the interspecies interactions. In Figs. 5, 6 and 7, we show the density of states for fermions for $n_{\rm f} = 0.5, 0.1, 0.9$ (or $n_{\rm b} = 0.5, 0.9, 0.1$), respectively, under the condition of $U_{\rm bf} = U_{\rm bb}$. From Fig. 5, it can be seen that there is finite quasiparticle density of states near the fermi energy level for relatively small values of $U_{\rm bf}$, and when $U_{\rm bf}$ is increased to 4.25 and above, the fermionic atoms in the optical lattice are shown in the Mott insulator state. Moreover, from Figs. 6 and 7, it is found that the Mott phase transitions for the two species (bosons and fermions) occur simultaneously at a certain critical point, regardless of the fermion composition.

Results on the ground-state properties of the bose-femi mixture calculated from the DMFT approach can also be reproduced by the Gutzwiller method, while dynamical quantities, such as those shown in Figs. 6 and 7, are not accessible by the Gutzwiller method. We note that the Gutzwiller approximation with the full set of

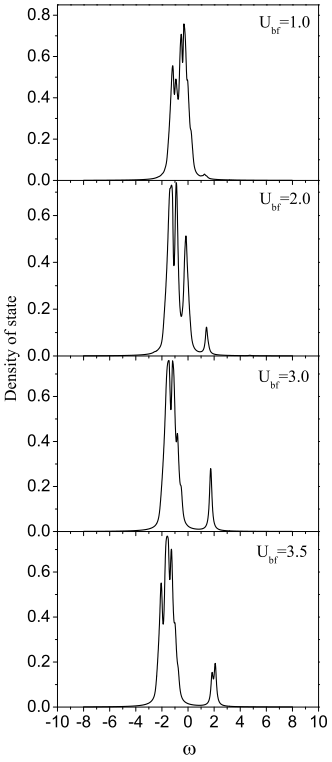

Fig. 7 Fermion density of states calculated by DMFT for $n_{\rm f} = 0.9$, $n_{\rm b} = 0.1$ and $U_{\rm bb} = U_{\rm bf}$. Four values of $U_{\rm bf}$, 1.0, 2.0, 3.0 and 3.5, are shown.

variational parameters is used here instead of its zero-order approximation which is equivalent to the slave-boson approach. Similar variational calculations with full sets of parameters have been applied to Holstein polarons with off-diagonal coupling [32]. We can make comparisons for the superfluid order parameter and the ground state energy for the case of $U_{\rm bf} = U_{\rm bb}$ and $n_{\rm b} = n_{\rm f} = 0.5$ by the two methods. Results are plotted in Fig. 8, in which it is found that the Gutzwiller approximation is almost as accurate as the DMFT method for determining the ground state properties of the bose-femi mixture. This point would be very important to investigations on

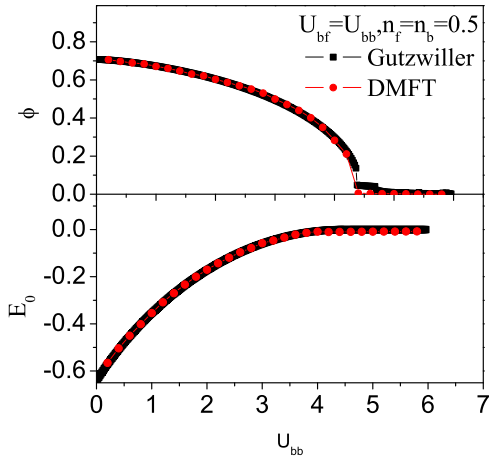

Fig. 8 The superfluid order parameter ϕ (upper panel) and the ground state energy E_0 (lower panel) as a function of $U_{\rm bb}$ calculated from the DMFT (red) and the Gutzwiller (black) methods for the case of $U_{\rm bf} = U_{\rm bb}$ and $n_{\rm b} = n_{\rm f} = 0.5$.

the cold-atom issues. Furthermore, in addition to the case of $n_{\rm b} + n_{\rm f} = 1$, there are other interesting situations to investigate the effects of adding fermions into the cold atomic mixtures, which are elaborated in the following subsection.

3.2 Effects of adding fermions

Whne the effect of adding fermions on the bosonic coherence is considered, the bose-fermi interaction $U_{\rm bf}$ turns out to be an important factor. In Fig. 9, we show that the quantum critical point of the bosonic Mott transition, $U^c_{\rm bb}$, as a function of the ratio $\gamma = U_{\rm bf}/U_{\rm bb})$, where the occupation numbers for bosons and fermions are fixed (double half-filling). It is demonstrated in Fig. 9 that different γ can lead to different $U^c_{\rm bb}$ in the formation of the superfluidity in comparison with the case of

pure bosons. When γ is less (greater) than 0.6, the critical value $U_{\rm bb}^c$ goes above (below) that of the pure-boson case, 5.8. We conclude that when a weak bose-fermi interaction is considered, addition of fermions results in disturbing the uniform distribution of bosons. It is equivalent to introduce some effective bosonic holes to the bosonic system. These bosonic holes favor the motion of bosons in the optical lattice. For strong bose-fermi interactions, the superfluid bosonic wave function can be severely scattered by the presence of fermions, impeding bosonic transport. Therefore, these two different fermion effects are observed in the formation of the bosonic superfluidity.

Next, we consider the case of $n_{\rm b} = 1$ and $U_{\rm bb} = 8$, which shows adding fermions can induce the superfluidity of bosons, a fact that is corroborated by the Gutzwiller method. As shown in Fig. 10, once $U_{\rm bf}$ exceeds a critical value, the superfluid order parameter becomes non-zero, and the quasi-particle weight $Z_{\rm f}$ for fermions begins to decrease. What is different in the lower panel of Fig. 10 is that bosons and fermions simultaneously enter the Mott phase at $U_{\rm bf} = 12$ due to formation of composite fermions consisting of one fermion and two bosonic holes [5], satisfying the Mott-transition condition as $1 \times n_{\rm f} + 1 \times (1 - n_{\rm f}) = n_{\rm b}$.

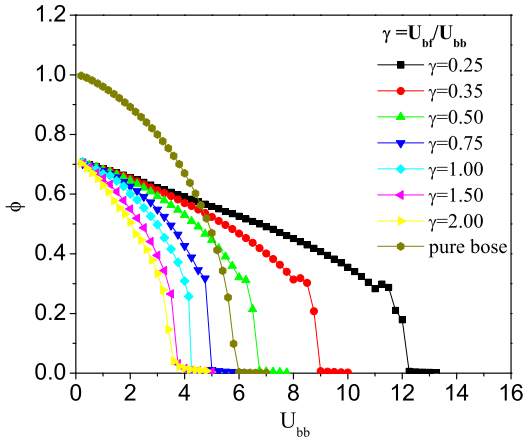

Fig. 9 The quantum critical point of the bosonic Mott transition $U_{\rm bb}^c$ as a function of the ratio γ ($\gamma = U_{\rm bf}/U_{\rm bb}$), and the occupation numbers for bosons and fermions is fixed as double half-filling.

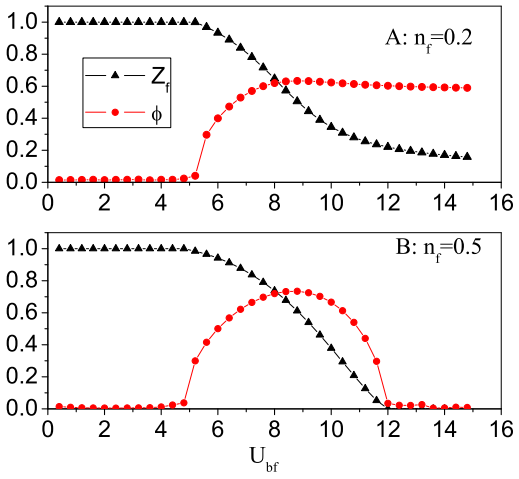

Fig. 10 The superfluid order parameter for bosons (red) and the quasi-particle weight for fermions (black) as a function of $U_{\rm bf}$ for $U_{\rm bb} = 8$, $n_{\rm b} = 1$, and two values of $n_{\rm f}$: (A) $n_{\rm f} = 0.2$ (upper panel); (B) $n_{\rm f} = 0.5$ (lower panel).

3.3 Particle distributions for inhomogeneous cases under local density approximation

In the previous subsection, we have demonstrated the effect of fermions on the bosonic superfluidity. A rich

phase diagram is expected after adding the fermions to the bosonic system. Here we present a phase diagram spanned by the chemical potentials $\mu_{\rm b}$ and $\mu_{\rm f}$ for the case of $U_{\rm bb} = U_{\rm bf} = 6$ in Fig. 11. Four regions labeled by I, II, III and IV represent the superfluid phase for pure bosons, the coexisting regions of superfluid bosons and fermion liquid, the Mott region, and the superfluid bosons with integer filling fermions, respectively. Along the diagonal line of Fig. 11, much less coexisting regions (type II) for the two species are found. The strong repulsive interaction $U_{\rm bf}$ leads to the phase separation of the mixture. As pointed out in Ref. [33] for a two-dimensional boson-fermion mixture, the main mechanism of the phase separation is a weak perturbation of the boson density inducing a modulation of the fermionic density. The fermionic distortion among the bosons induces an attractive interaction. Phase separation occurs when the induced attraction reaches the same order of magnitude as the intrinsic repulsion $U_{\rm bb}$ between bosons.

For ultracold atoms confined in an optical lattice, it is necessary to superimpose an extra external potential onto the optical lattice in order to generate an assemble of quantum degenerate atoms [12]. This external potential is a combination of a magnetic potential in which the condensate is initially formed and an optical one due to the Gaussian shape of the lattice beam [34]. The external potential can be approximated by one that is harmonic and isotropic, such as $V(r) = (m/2)\omega_t^2 r^2$, where m is the atomic mass, ω_t is trapping frequency, and r denotes

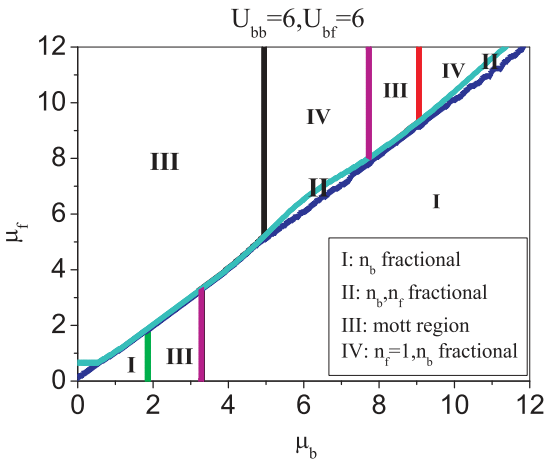

Fig. 11 The phase diagram of the bose-fermi mixture spanned by the chemical potentials $\mu_{\rm b}$ and $\mu_{\rm f}$ for the case of $U_{\rm bb} = 6$ and $U_{\rm bf} = 6$. Four regions labeled by I, II, III and IV, represent the superfluid phase for pure bosons, the coexisting regions of superfluid bosons and fermion liquid, Mott region, and superfluid bosons with integer filling fermions, respectively.

the lattice site distance from the trap center. An exact criterion for solving the inhomogenous bose-fermi mixture will involve calculating the Helmholtz free energy as a function of all eigenstates of the trapping potential. When the external potential varies slowly across the lattice, we can utilize the local-density approximation (LDA), and regard the globally inhomogenous system as being locally homogeneous [34,35]. After the functional relation $n_{\rm homo}(\mu)$ between the chemical potential μ and the particle distribution n is calculated from the aforementioned DMFT or Gutzwiller method for the homogeneous system, the density distribution for the inhomogeneous system can be evaluated by $n(r) = n_{\rm homo}(\mu - V(r))$. The chemical potential $\mu_{\rm b(f)}$ is related to the total

fermion (boson) number. It is noted that the LDA will break down at the edge of the ultracold-atom colony. In the following discussion, $(m/2)\omega_t^2$ takes a constant value of 0.09 along the radical direction.

In the upper four panels of Fig. 12, we display density profiles of the two species along the radial direction with $U_{\rm bb} = U_{\rm bf} = 6$ under the condition that the bosons are in the superfluid state completely prior to adding the fermions. The chemical potentials of the four cases are chosen as (a) $\mu_{\rm b} = 0.6, \mu_{\rm f} = 0.0$, (b) $\mu_{\rm b} = 0.7, \mu_{\rm f} = 0.77$, (c) $\mu_{\rm b} = 0.95, \mu_{\rm f} = 1.08$, and (d) $\mu_{\rm b} = 1.2, \mu_{\rm f} = 1.349$. From these density distributions, it can be seen that, when the bosons are in the superfluid state, the added fermions firstly fall into the center region, pushing bosons away from the trap center, and a further increase in the fermion composition drives the bosons around the central area into the Mott region. As shown in Panel (c) of Fig. 12, the fermions entering the coexisting region expels the bosons to the outer shell, and the central fermions are found at a composition plateau of 0.87, leaving the boson composition at 0.13. The coexistence of two species can result in new quantum phases such as charge density wave and supersolid [36,22]. The composition plateaux indicate that the bosons and the fermions are both in the Mott state. This is analogous to a shell-type structure of the bosonic density, in which the Mott-insulator phases are visible as integer plateau regions for purely boson systems [3,37].

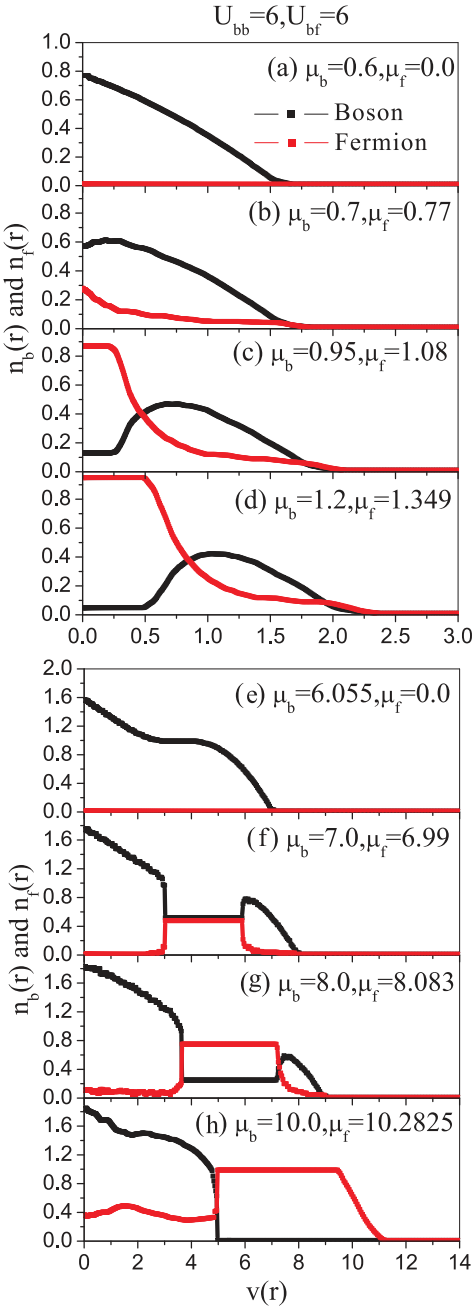

Fig. 12 Density profiles of bosons (black) and fermions (red) for $U_{\rm bb} = U_{\rm bf} = 6$. Panels (a)-(d): The bosons are in the superfluid state completely prior to adding the fermions; Panels (e)-(h): The bosons are partially in the Mott state prior to adding the fermions.

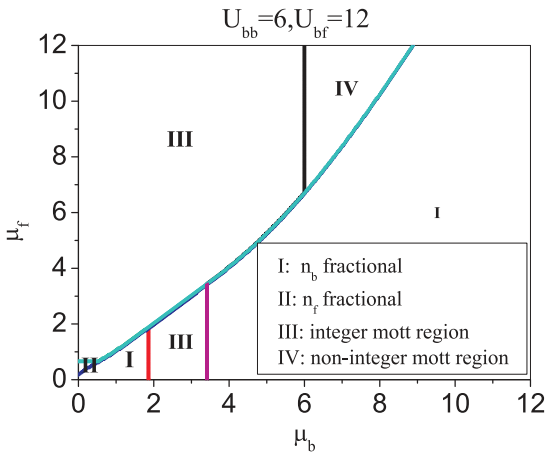

Fig. 13 The phase diagram of the bose-fermi mixture spanned by the chemical potentials $\mu_{\rm b}$ and $\mu_{\rm f}$ for the case of $U_{\rm bb} = 6$ and $U_{\rm bf} = 12$.

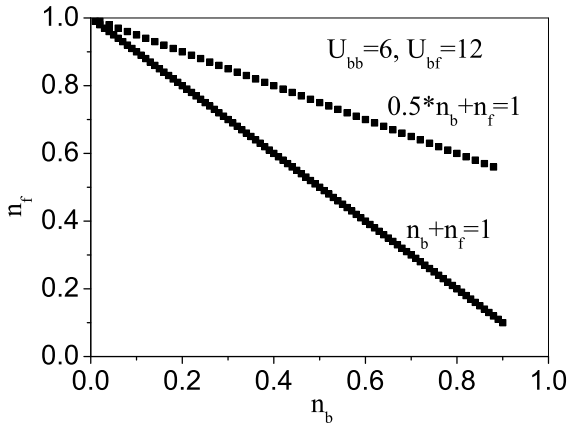

Fig. 14 The Mott phase transition point for $U_{\rm bb} = 6$, $U_{\rm bf} = 12$. The occurrence of the Mott phase transition satisfies $n_{\rm b} + n_{\rm f} = 1$ or $0.5n_{\rm b} + n_{\rm f} = 1$.

The lower four panels of Fig. 12 display density profiles of the two species along the radial direction under the initial condition that the bosons are partially in the Mott state prior to adding the fermions. Interaction strengths remain unchanged at $U_{\rm bb} = U_{\rm bf} = 6$. The chemical potential of the two species are set as (e) $\mu_{\rm b} = 6.055, \mu_{\rm f} = 0.0$, (f) $\mu_{\rm b} = 7.0, \mu_{\rm f} = 6.99$, (g) $\mu_{\rm b} = 8.0, \mu_{\rm f} = 8.083$, and (h) $\mu_{\rm b} = 10.0, \mu_{\rm f} = 10.2825$. It is found that the added fermions aggregate in the Mott region driving bosons towards two sides of the Mott region, and as a result, the bosonic superfluid density increases in the central region. As shown in Panel (f) of Fig. 12, there is a common plateau shared by the two species in the Mott region with a boson (fermion) composition of 0.52 (0.48). Panel (h) of Fig. 12 reveals the occurrence of phase separation in the bose-fermion mixture for a sufficiently fermion composition.

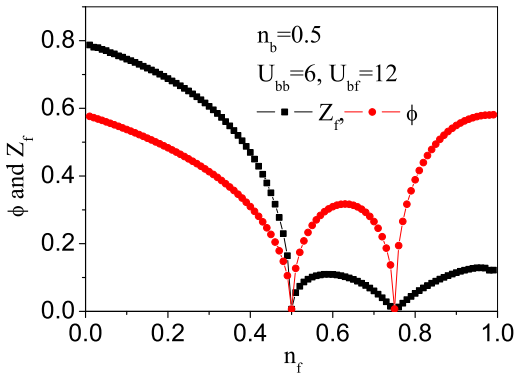

Fig. 15 The quasi-particle spectral weight $Z_{\rm f}$ (black) and the superfluid order parameter ϕ (red) as a function of the average number $n_{\rm f}$ for the case of $n_{\rm b} = 0.5$ and $U_{\rm bb} = 6, U_{\rm bf} = 12$. The bosons and the fermions simultaneously enter the Mott phase at $n_{\rm f} = 0.5$ and $n_{\rm f} = 0.75$.

In order to gain a deeper understanding and compare with experiment [8], we plot the phase diagram for the case of $U_{\rm bb} = 6$ and $U_{\rm bf} = 12$ in Fig. 13. Due to the presence of stronger boson-fermion repulsive interactions, Fig. 13 differs substantially from Fig. 11. First,

almost no coexistence of boson superfluid and fermion liquid is found, and Region II in Fig. 13 denotes the pure fermion liquid. Second, Region IV is still a Mott phase, where composite fermions made of one fermion and two bosonic holes are found with a non-integer total filling factor. This is to say, for the case of $U_{\rm bf} = 2U_{\rm bb}$, the prerequisite for the Mott phase transition is to satisfy $n_{\rm b} + n_{\rm f} = 1$ or $0.5n_{\rm b} + n_{\rm f} = 1$, as shown in Fig. 14. Furthermore, to further look into the Mott phase transition with a non-integer filling factor, we also calculate the quasi-particle spectral weight $Z_{\rm f}$ (for the fermions) and the superfluid order parameter ϕ (for the bosons) for the case of $n_{\rm b} = 0.5$, $U_{\rm bb} = 6$ and $U_{\rm bf} = 12$. The results are plotted in Fig. 15, wherein it is obvious that the bosons and fermions simultaneously enter the Mott phase at $n_{\rm f} = 0.5$ and $n_{\rm f} = 0.75$.

Lastly, we look into the real space distributions of bosons and fermions that correspond to the phase diagram in Fig. 13 for the case of $U_{\rm bb} = 6, U_{\rm bf} = 12$. The upper four panels of Fig. 16 display the effect of adding fermions into a superfluid bosonic system. The chemical potentials correspond the four panels are (a) $\mu_{\rm b} = 0.5, \mu_{\rm f} = 0.0$, (b) $\mu_{\rm b} = 0.6, \mu_{\rm f} = 0.695$, (c) $\mu_{\rm b} = 0.7, \mu_{\rm f} = 0.826$ and (d) $\mu_{\rm b} = 1.2, \mu_{\rm f} = 1.362$. When fermions enter the bosonic system, they prefer to stay in the center region. Further increasing the fermion composition leads to the formation of the Mott region such as that in Panel(d) of Fig. 16, where the fermion (boson) composition is 0.96 (0.04). The lower four panels of

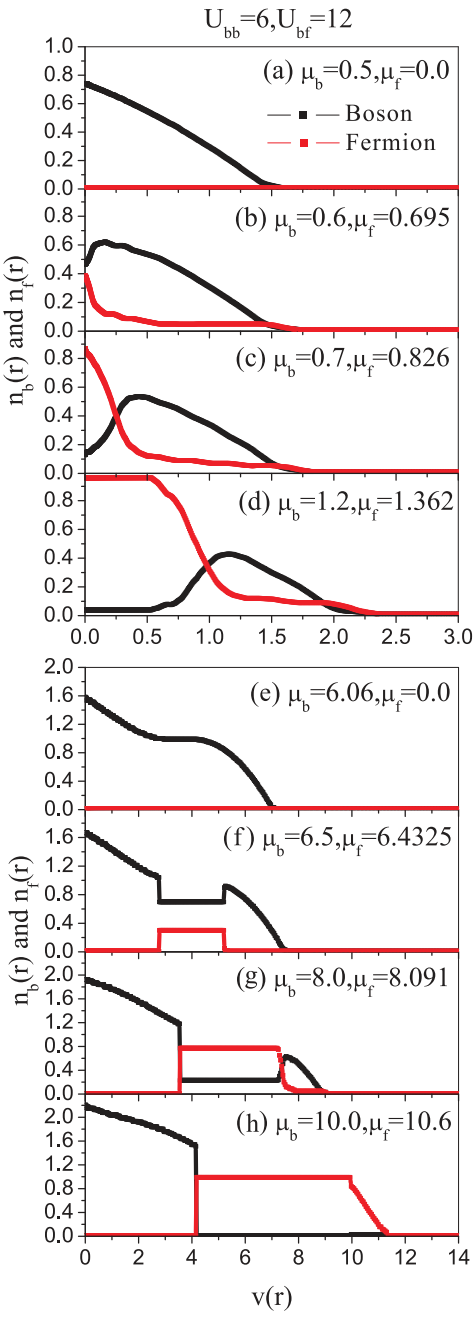

Fig. 16 Density profiles of bosons (black) and fermions (red) for $U_{\rm bb} = 6$ and $U_{\rm bf} = 12$. Panels (a)-(d): The bosons are in the superfluid state completely prior to adding the fermions; Panels (e)-(h): The bosons are partially in the Mott state prior to adding the fermions.

Fig. 16 display the density profiles of the two species under the condition that the bosons are initially in a Mott insulator state. It is found that the added fermions enter the Mott region, driving the bosons in the center region toward two sides of the Mott plateau. The corresponding chemical potentials for the four panels are set as (e) $\mu_{\rm b} = 6.06, \mu_{\rm f} = 0.0$, (f) $\mu_{\rm b} = 6.5, \mu_{\rm f} = 6.4325$, (g) $\mu_{\rm b} = 8.0, \mu_{\rm f} = 8.091$ and (h) $\mu_{\rm b} = 10.0, \mu_{\rm f} = 10.6$. As compared with Fig. 12 ($U_{\rm bf} = 6$), much less overlap of boson superfluid and fermion liquid can be found in Fig. 16 ($U_{\rm bf} = 12$). Complete separation between the bosons and the fermions in real space is found for $\mu_{\rm b} = 10.0, \mu_{\rm f} = 10.6$ as clearly demonstrated in Panel (h) of Fig. 16.

Thermal effects in the cold-atom systems are of extreme importance. Although the numerical approaches employed in the present paper are only valid for probing the ground state properties, we can still use them to gain some insight into the thermal effects. For example, temperature can modify the density profile discussed in the previous section. This is because in the region where bosons are mixed with fermions, there are more low energy excitations due to the presence of the Fermi surface than in the boson-only region. The boson-fermion mixing will generate additional configurational entropy at finite temperatures and thus lower the free energy. Therefore, compared to the boson-only region, the area where bosons mingle with fermions will be more stable at elevated temperatures due to the entropic effect, and is expected to expand in size with increasing temperature.

4 Conclusion

In summary, we have investigated a strongly correlated bose-fermi mixture in a three-dimensional optical lattice at zero temperature by the DMFT and the Gutzwiller approximation. By examining the effect of added fermions on the bosonic coherence, we conclude that, in a bosonic insulator with integer filling factors, fermions will destroy the MI state of bosons only if the bose-fermi coupling interaction is sufficiently strong. However, if the added fermions are bound with one or more bosonic holes uniformly distributed throughout the optical lattice, the impact of the fermions relies on the bose-fermi interaction; e.g., for the case of one fermion combined with one bosonic hole, the critical value of the bose-fermi interaction is $0.6U_{\rm bb}$. For the experimental case with $U_{\rm bf} = 2U_{\rm bb}$ [8], our study shows fermion addition will destroy the superfluidity of the bosons. Our work provides a theoretical basis for future experimental verfication of the role of fermions on the bosonic coherence in the bose-fermi mixtures.

In addition, we have shown several possible phases and density profiles for the bose-fermi mixture with repulsive interactions $U_{\rm bf}$. It is concluded that, when the bosons are in the superfluid state, the added fermions tend to bind with the bosonic holes, resulting in the formation of a Mott phase in the center region. While as the

bosons have a plateau distribution, the added fermions preferentially fall into the Mott regions, and stay with bosonic holes. A further increase in the fermion number leads to a higher value of superfluid fraction for bosons at the center region, simultaneously pushing bosons to further extend. Once some fermions are bound with two or three bosonic holes, another Mott plateau will appear. Although our study in this paper is focused on fermion-boson mixtures with repulsive interactions, it is not hard to map our problem to a similar one with attractive interactions by applying the particle-hole transformation to the fermions. Therefore, the results obtained in this paper can be readily applied to the fermion-boson system with attractive interactions as well [21]. Analysis of the phase separation and the coexistence for the bose-fermi mixtures in this work will add to our fundamental understanding of the atomic gases in future studies of novel quantum phases.

Acknowledgments

This work is supported in part by the NSF of China under grant No. DMR-0404252 and DMR-0606485 (X.D.) and by the NSFC under the grant No. 90303022, 60576058, 10334090 and 10425418 (Z.F.). Support from the Singapore Ministry of Education through the Academic Research Fund (Tier 2) under Project No. T207B1214 is also gratefully acknowledged (Q.M.L.). One of us (Y.Z.) would like to thank Jianhui Dai for useful discussion.

References

1. M. Köhl, H. Moritz, T. Stöferle, K. Günter and T. Esslinger, Phys. Rev. Lett. **94**, 080403(2005).
2. C. Chin, M. Bartenstein, A. Altmeyer, S. Riedl, S. Jochim, J. H. Denschlag, and R. Grimm, Science **305**, 1128(2004).
3. D. Jaksch, C. Bruder, J. I. Cirac, C. W. Gardiner, and P. Zoller, Phys. Rev. Lett. **81**, 3108(1998).
4. M. Greiner, O. Mandel, T. Esslinger, T. Hansch, and I. Bloch, Nature **415**, 39(2002).
5. M. Lewenstein, L. Santos, M. A. Baranov and H. Fehmann, Phys. Rev. Lett. **92**, 050401(2004).
6. K. Sengupta, N. Dupuis, and P. Majumdar, Phys. Rev. A **75**, 063625(2007)
7. S. Ospelkaus, C. Ospelkaus, O. Wille, M. Succo, P. Ernst, K. Sengstock, and K. Bongs, Phys. Rev. Lett. **96**, 180403(2006).
8. K. Günter, T. Stöferle, H. Moritz, M. Köhl, and T. Esslinger, Phys. Rev. Lett. **96**, 180402(2006).
9. L. Pollet, C. Kollath, U. Schollwöck, and M. Troyer, Phys. Rev. A **77**, 023608 (2008).
10. M. Cramer, S. Ospelkaus, C. Ospelkaus, K. Bongs, K. Sengstock and J. Eisert, Phys. Rev. Lett. **100**, 140409 (2008).
11. C. Ospelkaus, Fermi-bose mixtures: from mean-field interactions to ultracold chemistry, Ph.D. thesis.
12. S. Ospelkaus, Quantum Degenerate Fermi-Bose Mixtures of 40K and 87Rb in 3D optical lattice, Ph.D. thesis.
13. A. Georges, G. Kotliar, W. Krauth and M. J. Rozenberg, Rev. Mod. Phys. **68**, 13(1996).

14. J. Bünemann, and W. Weber, Phys. Rev. B **57**,6896(1998)
15. M. C. Gutzwiller, Phys. Rev. Lett. **10**, 159 (1963); M. C. Gutzwiller, Phys. Rev. **134**, A923 (1964); M. C. Gutzwiller, Phys. Rev. **137**, A1726 (1965).
16. R. Roth and K. Burnett, Phys. Rev. A **67**, 031602 (2003).
17. S.J. Gu *et al.*, Phys. Rev. B **102**, 224508 (2009).
18. , L. Pollet *et al.*, Phys. Rev. Lett. **96**, 190402 (2006).
19. X. Y. Deng, L. Wang, X. Dai and Z. Fang, Phys. Rev. B **79**, 075114(2009).
20. A. Albus, F. Illuminati, and J. Eisert, Phys. Rev. A **68**, 023606 (2003).
21. Th. Best, S. Will, U. Schneider *et al.*, Phys. Rev. Lett. **102**, 030408 (2009).
22. I. Titvinidze, M. Snoek, and W. Hofstetter, Phys. Rev. Lett. **100**, 100401 (2008).
23. L. Amico,and V. Penna, Phys. Rev. Lett. **80**, 2189(1998).
24. K. Sheshadri, H. R. Krishnamurthy, R. Pandit, and T. V. Ramakrishnan, Europhys. Lett. **22**, 257(1993).
25. C. Raas, G. S. Uhrig, and F. B. Anders, Phys. Rev. B **69**(4), 041102(R)(2004); C. Raas and G. S. Uhrig, Eur. Phys. J. B 45(3), 293-303 (2005).
26. G. Kotliar and A. E. Ruchenstein, Phys. Rev. Lett. 57, 1362(1986)
27. X. Dai, G. Kotliar, Z. Fang, arXiv:cond-mat/0611075
28. R. Fresard and G. Kotliar, Phys. Rev. B 56, 12909 (1997); H. Hasegawa, Phys. Rev. B 56, 1196, (1997).
29. L. Pollet, S. M. A. Rombouts, and P. J. H. Denteneer, Phys. Rev. Lett. **93**, 210401(2004).
30. B. Paredes, A. Widera, V. Murg, and et al, Nature **429**, 277(2004).
31. M. P. A. Fisher, P. B. Weichman, G. Grinstein, and D. S. Fisher, Phys. Rev. B **40**, 546(1989).
32. Q.M. Liu, Y Zhao, W.H. Wang, T. Kato, Phys. Rev. B **79**, 165105 (2009).
33. H. P. Büchler, and G. Blatter, Phys. Rev. A **69**, 063603(2004)
34. F. Gerbier, A. Widera, S. Fölling, O. Mandel, T. Gericke, and I. Bloch, Phys. Rev. A **72**, 053606(2005)
35. X. X. Yi, and C. P. Sun, Phys. Rev. A **64**, 043608(2001).
36. F. Hert, G. G. Batrouni, X. Roy, and V. G. Rousseau, Phys. Rev. B **78**, 184505 (2008).
37. M. Greiner, Ultracold quantum gases in three-dimensional optical lattice potentials, Ph.D. thesis, 2003.